The KLOE-2 experiment at DAΦNE

Antonio De Santis‡

INFN - Laboratori Nazionali di Frascati, v. Enrico Fermi, 50, 00044

E-mail: antonio.desantis@lnf.infn.it

September 2016

Abstract. The KLOE-2 experiment is currently collecting data at DAΦNE the INFN e^+e^- collider located in the Frascati National Laboratories. In the two DAΦNE main rings, electrons and positrons are stored to collide at a center of mass energy of 1.02 GeV, the ϕ mass resonance. The KLOE-2 have already collected 2.4 fb^{-1} integrated luminosity that corresponds to 7.4 billion of ϕ decays recorded. The goal of the KLOE-2 physics run is to collect at least 5 fb^{-1}before the end of 2017.

The KLOE-2 experiment has a wide physics program ranging from discrete symmetries test to the study of light unflavored mesons produced by the radiative decay of the ϕ mesons while searching for light mass exotic candidates for the dark matter problem. In order to face this huge program a deep revision of the original KLOE apparatus has been performed.

In this contribution the upgrade of the detector will be briefly discussed before starting a more detailed presentation on some results concerning: CPT and Lorentz Invariance tests with neutral kaons, dark forces massive boson mediator searches, hadron structure and low energy mesons interaction.

1. Present status

The KLOE-2 experiment [1] is currently taking data at DAΦNE collider [2, 3], the e^+e^- accelerator of the Frascati National Laboratory running at the ϕ resonance peak. DAΦNE began operations for KLOE-2 experiment in November, 2014 with a new interaction region [4]. Several consolidation intervention [5, 6, 7] allowed to deliver 3.0 fb^{-1} of integrated luminosity to the KLOE-2 experiment that collected 2.4 fb^{-1}on mass storage system. The progression along the time of the data delivery is shown in fig. 1.

A record peak-luminosity of 2.21×10^{32} cm^{-2}s^{-1} has been achieved. The daily best luminosity delivered has been 13.4 pb^{-1} and a weekly best integrated luminosity of 76.3 pb^{-1}has been observed.

2. KLOE-2 experimental apparatus

The KLOE-2 experiment is an upgraded version of the previous KLOE apparatus with the inclusion of new sub-detectors allowing for larger physics program with increased reconstruction performance.

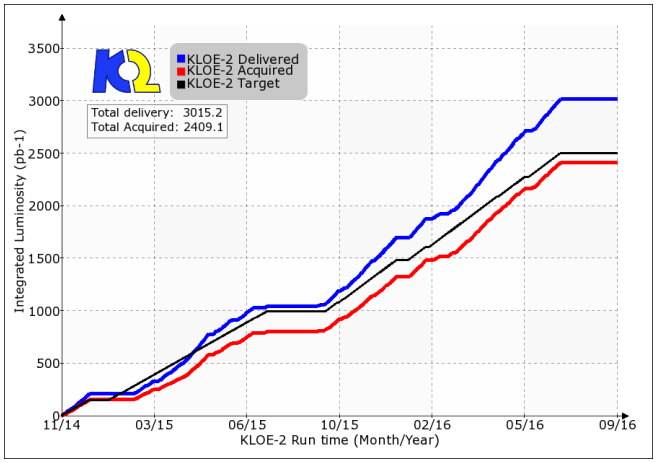

Figure 1. The time evolution of the DAΦNE data delivery since November, 2014. The blue line represent the integrated luminosity delivered, while the red curve is the corresponding amount of integrated luminosity acquired. The black line represent the target luminosity fixed to achieve the KLOE-2 goal of 5 fb^{-1} by the end of KLOE-2 physics run. The black line is horizontal during DAΦNE planned shut-downs (maintenance/laboratory closure).

The original KLOE detector consists of a large cylindrical drift chamber (DC) surrounded by a lead-scintillating fiber electromagnetic calorimeter (EMC). A super-conducting coil around the EMC provides a 0.52 T axial field.

The DC [8] is 4 m in diameter and 3.3 m long and has 12,582 all-stereo cells properly arranged in 58 layers to ensure homogeneous detector response. Time and amplitude of signals from cells are read-out to measure hit positions and energy loss. The position resolutions for single hits are $\sigma_{r,\phi}\sim$150 μm and $\sigma_z\sim$2 mm in the transverse and longitudinal plane, respectively and are almost homogeneous in the active volume. The momentum resolution is $\sigma(p_\perp)/p_\perp \sim 0.4\%$ for polar angles in the range $40° - 130°$.

The EMC [9] is divided into a barrel and two end-caps covering 98% of the solid angle. Signals from impinging particles are read out by photo-multipliers and amplitudes and time of the signals are recorded. Energy and time resolutions are $\sigma_E/E_{\rm clu} = 5.7\%/\sqrt{E_{\rm clu}({\rm GeV})}$ and $\sigma_{T_{\rm clu}} = 57{\rm ps}/\sqrt{E_{\rm clu}({\rm GeV})} \oplus 100$ ps, respectively.

The KLOE-2 experimental program [1] implies several detector improvements in order to increase the physics results outcomes.

For the gamma-gamma physics two pairs of electron-positron taggers have been installed: a small LYSO crystal calorimeter matrix, the Low Energy Tagger [10] inside the KLOE apparatus and a plastic

‡ on behalf of KLOE-2 Collaboration

scintillator hodoscope, the High Energy Tagger (HET) [11], along the beam lines outside the KLOE detector. The fig. 2 shows the status of the HET commissioning. The observed counting rate of HET stations have been described in terms of beam loss due to Toushek scattering and beam-beam effective scattering in the interaction region.

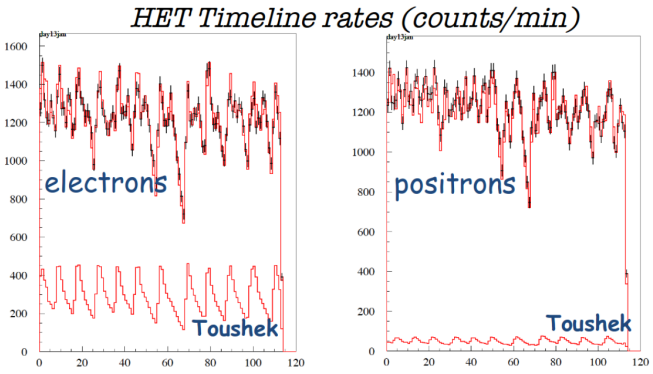

Figure 2. HET electron (left) and positron (right) counts as a function of the time (2 hr total) during collisions. The observed shapes have been described in terms of background due to Toushek scattering inside the beam and KLOE-2 trigger components. In the electron case the background accounts for 20-30% of the total observed rate while for positrons is below 8%.

To improve the acceptance and the angular coverage two new calorimeters have been developed. A pair of LYSO crystal calorimeters (CCALT) [12] have been installed near the interaction region to improve the angular acceptance for low-θ particles. This calorimeter will be also useful to provide fast signals for luminosity measurement and beam instability feedback to help DAFNE tune-up.

A pair of tile calorimeters (QCALT) [13], covers the quadrupoles inside the KLOE detector and along the beam pipe. These calorimeters are made of tungsten slabs and singly read-out scintillator tiles to improve the angular coverage for particles coming from the active volume of the DC (e.g. K_L decay).

In order to increase the resolution on the vertex reconstruction for decay in the vicinity of the primary interaction point a small and light inner tracker (IT) [14] made of four planes of cylindrical GEM have been designed. The alignment and calibration of this detector is shown in fig. 3

During data taking the DAΦNE beam conditions and detector calibrations are constantly monitored in order to guarantee the highest quality of the collected data.

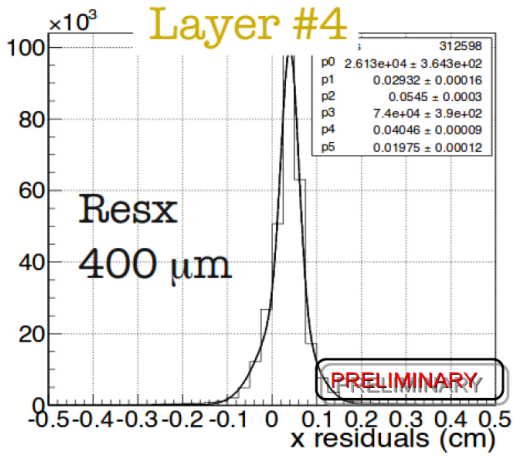

Figure 3. Residuals between observed and projected impact point with Bhabha scattering events on the outermost plane of the IT. The width of this distribution is the convolution of the IT and DCH resolutions.

3. Kaon interferometry

The ϕ mesons produced at the DAΦNE ϕ-factory have a small residual momentum in the horizontal plane and the branching fraction for the ϕ decay in neutral kaon pair is 34%. This decay preserves the ϕ quantum numbers ($J^{PC} = 1^{--}$) resulting in a anti-symmetric combination of the two kaon mass eigenstate:

$$|\phi\rangle \propto |\mathrm{K_S}, \vec{p}\rangle|\mathrm{K_L}, -\vec{p}\rangle - |\mathrm{K_S}, -\vec{p}\rangle|\mathrm{K_L}, \vec{p}\rangle$$

The time evolution of the kaon system preserves the initial correlation. Labelling f_1 and f_2 the final decay channels for the two kaons and evaluating the probability of a decay into $|f_1, f_2\rangle$ final state as a function of the difference of decay times (Δt) the following equation can be obtained [15]:

$$I_{f_1 f_2}(\Delta t) \propto e^{-\Gamma_\Sigma |\Delta t|}\Big[|\eta_{f_1}|^2 e^{\frac{\Delta\Gamma}{2}\Delta t} + |\eta_{f_2}|^2 e^{-\frac{\Delta\Gamma}{2}\Delta t} - 2\Re e\Big(\eta_{f_1}\eta^*_{f_2} e^{-i\Delta m \Delta t}\Big)\Big] \quad (1)$$

where $\eta_{f_j} = \langle f_j|\mathrm{K_L}\rangle/\langle f_j|\mathrm{K_S}\rangle$, $\Gamma = \Gamma_S + \Gamma_L$ and $\Delta\Gamma = \Gamma_S - \Gamma_L$. Eq. 1 shows a time interference term characteristic of the so-called EPR correlation [16].

Choosing the same final state for both kaons in the event a fully destructive interference is expected for equal decay times ($|\Delta t| = 0$). The ratio of neutral kaon decay amplitudes (η_j) becomes:

$$\eta_j = \eta_{\pi^+\pi^-} = \frac{\langle\pi^+\pi^-|T|\mathrm{K_L}\rangle}{\langle\pi^+\pi^-|T|\mathrm{K_S}\rangle} \simeq \varepsilon_K + \varepsilon' - \delta_K \quad (2)$$

where ε_K is the CP violation parameter in the mixing, ε' is the direct CP violation parameter and δ_K stands for the amount of CPT violation in the kaon system. According to the Standard Model Extension

(SME) framework [17] and Greenberg theorem [18], the δ_K parameter is expressed as:

$$\delta_K \approx i \sin\phi_{SW} e^{i\phi_{SW}} \gamma_K (\Delta a_0 - \vec{\beta}_K \cdot \Delta\vec{a})/\Delta m, \qquad (3)$$

where γ_K and β_K are the usual Lorentz factors for the kaon, ϕ_{SW} is the super-weak phase and Δa_μ are the SME parameters for the kaon system that explicitly violates Lorentz endurance and triggers CPT violation.

Eq. 3 shows that δ_K is modulated by the kaon momentum modulus (γ_K and $|\vec{\beta}_K|$) and by its spatial direction ($\vec{\beta}_K$). In the KLOE case the two kaons are produced almost back-to-back in the ϕ decay and therefore evolve with two different δ_K ($\delta_K(\vec{P}_1) \neq \delta_K(\vec{P}_2)$). Additional angular dependence in the eq. 1 through eq. 3 is induced by the Earth motion (sidereal time variation) and residual ϕ momentum in the lab frame. The effect produced by CPT violation can be observed if the two kaon final states are identified with respect to their direction of propagation with respect to the fixed stars (see [17] equation 14). Two decay vertices reconstructed from the two pion tracks are selected and the decay length are transformed in proper decay time to construct the eq. 1 distribution. The data distributions have been fitted including SME effects to extract Δa_μ as show in fig. 4

The results for the Δa_μ parameters are [19]:

$$\begin{aligned}
\Delta a_0 &= (-6.0 \pm 7.7_{stat} \pm 3.1_{syst}) \times 10^{-18}\ \text{GeV},\\
\Delta a_X &= (\ 0.9 \pm 1.5_{stat} \pm 0.6_{syst}) \times 10^{-18}\ \text{GeV},\\
\Delta a_Y &= (-2.0 \pm 1.5_{stat} \pm 0.5_{syst}) \times 10^{-18}\ \text{GeV},\\
\Delta a_Z &= (\ 3.1 \pm 1.7_{stat} \pm 0.5_{syst}) \times 10^{-18}\ \text{GeV}.
\end{aligned}$$

These results constitute the most precise result in the quark sector of the SME. The total error is fully dominated by the statistical uncertainty.

CPT symmetry test are not limited to the SME framework. A very rich program of measurement using the interferometric approach is currently on-going. A study of the time evolution of CPT conjugate states will allow very clean and strong test of CPT violation as described in [20].

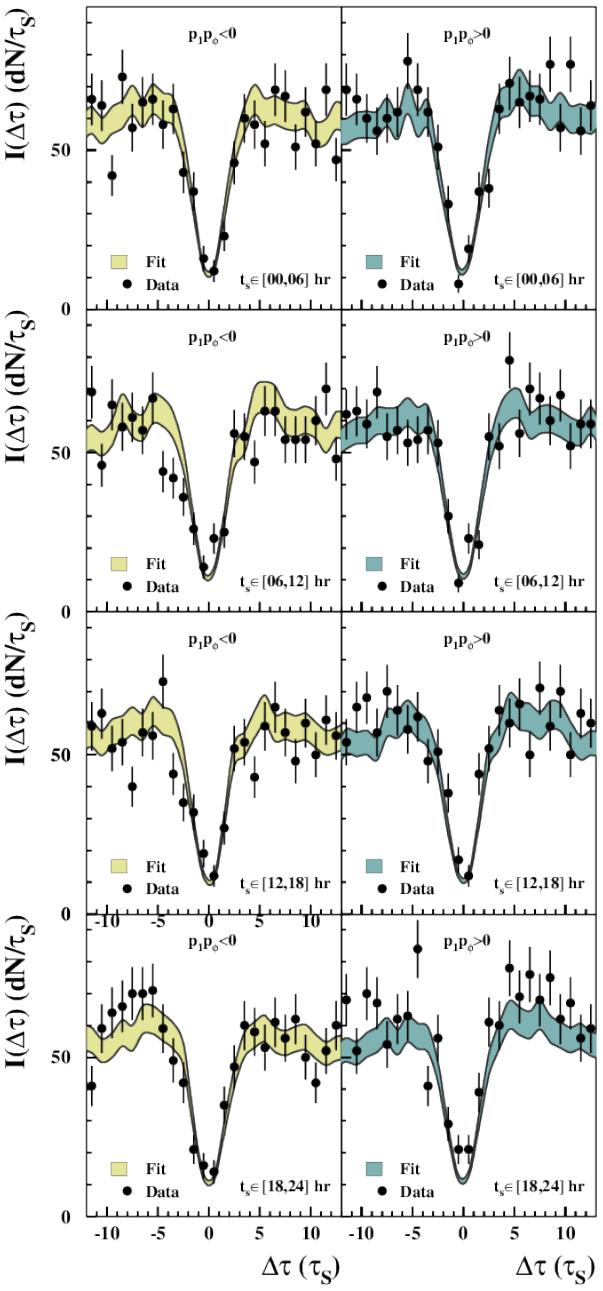

Figure 4. Fit results for Δa_μ parameters. left and right columns are relative to different angular selection in the laboratory frame while rows refers to different sidereal time interval. Black points are data while colored bands are the fit output. The fit χ^2/N_{DoF} is 211.7/187 corresponding to a probability of 10%.

4. Dark forces searches

Astrophysical observations have obtained results not fitting the Standard Model (SM) framework [21, 22, 23, 24, 25, 26, 27] and [28, 29, 30, 31]. To explain these anomalies a new gauge U(1) interaction mediated by a massive vector gauge boson, the U boson (dark photon), that kinetically mix with the SM U(1) hypercharge gauge field has been proposed. The mass of U boson is expected to be less than two proton masses to be compatible with the unaltered anti-proton astrophysical flux observed.

The small coupling between dark matter and the SM is described by a single kinetic mixing parameter: $\epsilon(= \alpha_D/\alpha_{EW})$. The resulting Lagrangian would be:

$$\mathcal{L}_{mix} = -\frac{\epsilon}{2} F^{EW}_{\mu\nu} F^{\mu\nu}_{Dark}$$

Depending on the interaction type, the U bosons should appear as a sharp resonance at m_U in the invariant-mass distributions of final-state particles in

reactions of the type $e^+e^- \to U\gamma$ with $U \to X^+X^-(X = e/\mu/\pi)$ or in meson Dalitz decays.

At KLOE two different searches were performed using the decay chain $\phi \to \eta U$ with $U \to e^+e^-$ and $\eta \to \pi^+\pi^-\pi^0$ [32] and $\eta \to \pi^0\pi^0\pi^0$ [33] as suggested in [34]. The two analyses selected a final sample of $\sim$ 13000 and $\sim$ 31000 events, respectively, using 1.7 fb^{-1}of data. Irreducible background from Dalitz decay $\phi \to \eta e^+e^-$ was studied separately, as discussed in the next section. A resonant peak was not observed and the CLS technique was used to set an upper limit on the strength of kinetic mixing parameter as a function of the U boson mass [35]. The 90% confidence level limit is shown in fig. 5.

Using 239.3 pb^{-1} of data a search for the U boson in the process $e^+e^- \to U\gamma$ with $U \to \mu^+\mu^-$ has been performed [36]. The signal appear as a narrow resonance in the final state dilepton invariant-mass spectrum. For this analysis the two charged tracks are required to be emitted at large-angle such that their energy is deposited in the barrel of EMC. The initial-state radiation (ISR) photon is not detected and was reconstructed using kinematics of the charged leptons. The final invariant mass spectrum was obtained after subtracting residual background and correcting for efficiency and luminosity. No resonant peak was observed so the CLS technique was used to estimate the maximum number of U boson signal events that can be excluded at 90% confidence level, N_{CLS}. In the estimate a systematic uncertainty of $\sim$ 1.5% has been taken into account. From N_{CLS} it is possible to estimate a limit on the kinetic mixing parameter:

$$\epsilon(m_{\mu\mu}) = \frac{\alpha_D}{\alpha_{EW}} = \frac{N_{CLS}(m_{\mu\mu})}{\varepsilon_{eff}(m_{\mu\mu})} \frac{1}{H(m_{\mu\mu})I(m_{\mu\mu})\mathcal{L}_{int}} \quad (4)$$

where the radiator function, $H(m_{\mu\mu})$, was evaluated with a MC dedicated simulation based on PHOKARA and $\mathcal{L}_{int} = 239.3\text{pb}^{-1}$ is the integrated luminosity and $\varepsilon_{eff}(m_{\mu\mu})$ ranges between 1%-10%. The 90% confidence level limit is shown in fig. 5.

The search of $U \to \mu^+\mu^-$ is obviously limited to U boson masses with $m_U > 2m_\mu$. To scan for lower values a search in the e^+e^- final state has been performed [47]. In this case, to have enough statistics around the threshold ($m_{ee} = 2m_e$), the event selection has been performed by selecting the ISR photon and leptons emitted at large angle (detected in the barrel). The resulting background contamination was less than 1.5%. No resonant U boson peak was observed prompting another use of the CLS technique to estimate N_{CLS}, the number of U boson signal events excluded at 90% confidence level. We used eq. 4 with $m_{\mu\mu} \to m_{ee}$ to set a limit on the kinetic mixing parameter as a function of m_U. For this analysis ε_{eff} ranges between 1.5% and 2.5%, and the $\mathcal{L}_{int} = 1.54$ fb^{-1} from 2004-05 KLOE data.

Further improvement with respect to previous results for m_U ranging between 500 and 1000 MeV has been obtained with the selection of the $\pi^+\pi^-\gamma$ final state [48]. The selection of the data is similar to the $\mu^+\mu^-\gamma$ final state. No evidence of peak in the di-pion invariant mass spectrum has been found. Comparing data distribution with the spectrum generated with the PHOKARA monte-Carlo event generator a N_{CLS} upper limit on the number of events as a function of the dipion invariant mass has been obtained. All the discussed results are shown in fig. 5.

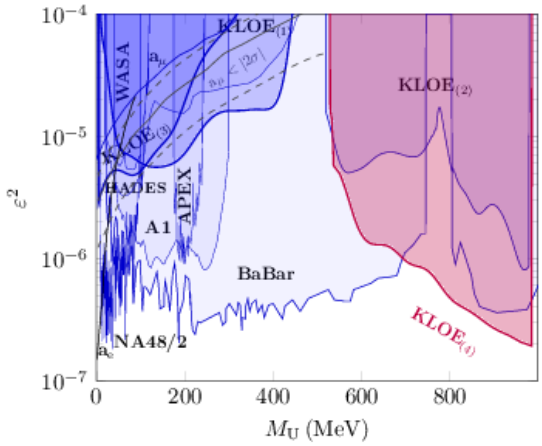

Figure 5. Summary of 90% CL exclusion limits on the dark sector coupling as a function of the U boson invariant mass. In the plot label KLOE(1) is for the combination of the results relative to $\phi \to \eta\gamma$ [32, 33], KLOE(2) and KLOE(3) is relative to $\mu^+\mu^-\gamma$ [36] and $e^+e^-\gamma$ [47] final state, respectively. KLOE(4) is for the $\pi^+\pi^-\gamma$ final state [48]. KLOE-2 results are also compared with the exclusion plots obtained by other experiments [38]-[45].

Different scenario is possible when the U(1) gauge symmetry is spontaneously broken by a Higgs-like mechanism, thus implying the existence of at least one other scalar particle, h' [46]. The hypothetical dark Higgs-strahlung process $e^+e^- \to Uh'$ with $U \to \mu\mu$ has been investigated using KLOE data [49]. The amplitude of this reaction is proportional to ϵ instead of ϵ^2 as for the previous process implying the possibility to set lower limits with the same amount of statistics. The production cross section of this process would be proportional to the product of the dark coupling and the kinetic mixing strength $\alpha_D \times \epsilon^2$. Assuming $m_{h'} < m_U$ the dark Higgs boson would have a large lifetime and escape KLOE-2 detector without interacting. 1.65 fb^{-1} of data collected at the ϕ-peak energy, and 0.2 fb^{-1} of data at 1 GeV energy have been used. Mass resolutions are 1 MeV for $m_{\mu\mu}$ (m_U) and 10 MeV for the missing mass ($m_{h'}$). A sharp peak in the two-dimensional distribution missing mass versus $m_{\mu\mu}$ is expected for the signal. The evaluation of background in every bin has been performed using the surrounding

bins to rescale montecarlo simulated distributions. The selection efficiency ranges between 15% and 25% and a conservative estimate of 10% systematic contribution has been taken into account. No evidence of the dark Higgs-strahlung process was found. Using uniform prior distributions, 90% confidence level Bayesian upper limits on the number of events, $N_{90\%}$, were derived separately for the two samples used and then combined. The coupling can be extracted from:

$$\alpha_D \times \epsilon^2 = \frac{N_{90\%}}{\varepsilon_{eff}} \frac{1}{\sigma_{Uh'}(\alpha_D\epsilon^2 = 1).\mathcal{L}_{int}} \quad (5)$$

where $\mathcal{L}_{int}$ is the integrated luminosity and $\sigma_{Uh'} \propto \frac{1}{s}\frac{1}{(1-m_U^2/s)^2}$ is the total cross section evaluated in the assumption $\alpha_D\epsilon^2 = 1$. The combined 90% confidence level limits are shown fig. 6.

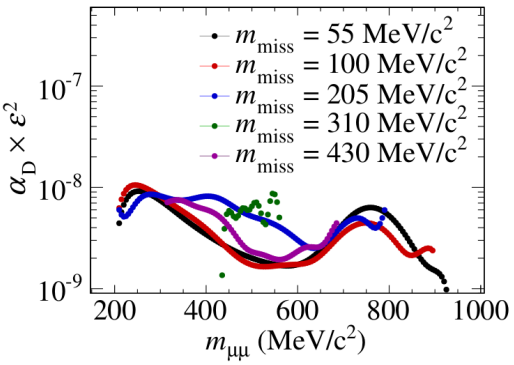

Figure 6. Limits from dark Higgs-strahlung process. The limit is presented as a function of the dilepton invariant mass (m_U) for different values of the event missing mass (dark Higgs mass). Lines represents the exclusion plots at the 90% CL.

5. Transition form factor

The low-energy structure of hadrons is strongly connected with precise knowledge of meson transition form factors (TFF) that are also connected in the determination of the "light-by-light" contribution to the anomalous magnetic moment of the muon, one the largest source of uncertainty in the $(g-2)_\mu$ calculation [50].

KLOE-2 collaboration has measured the $\phi \to \eta$ and $\phi \to \pi^0$ TFFs studying the decays $\phi \to \eta(3\pi^0)e^+e^-$ [53] and $\phi \to \pi^0 e^+e^-$ [54]. In fig. 7 the TFFs are shown as a function of $\sqrt{q^2} = m_{ee}$, the invariant mass of e^+e^- system. The observed mass spectrum has been described according to [51] where the TFF is included with a single pole parametrization, $|F_{\phi\eta}(q^2)|^2 := \frac{1}{1-q^2/\Lambda^2}$. The Λ parameter is extracted from the m_{ee} invariant mass spectrum and the corresponding slope parameter ($b_{\phi\eta} = \frac{dF(q^2)}{dq^2}|_{q^2=0} = \Lambda^{-2}$) is evaluated. The value $b_{\phi\eta} = 1.17 \pm 0.10^{+0.07}_{-0.11}\,\mathrm{GeV}^{-2}$ has been obtained while $1\mathrm{GeV}^{-2}$ is expected by pure VMD description. In the analysis has been measured also the branching fraction $B(\phi \to \eta e^+e^-) = 1.075 \pm 0.007 \pm 0.038) \times 10^{-4}$.

For the decay $\phi \to \pi^0 e^+e^-$, using the same parametrization [51], the invariant mass spectrum has been fitted and a slope of $b_{\phi\pi^0} = 2.02 \pm 0.11\,\mathrm{GeV}^{-2}$ has been obtained. Naive VMD extimate would give $b_{\phi\pi^0} \sim 1\,\mathrm{GeV}^{-2}$, while prediction based on disperve calculation [55] are $b_{\phi\pi^0} \sim 2.52 \ldots 2.68\,\mathrm{GeV}^{-2}$.

The branching fraction $B(\phi \to \pi^0 e^+e^-) = (1.035 \pm 0.005^{+0.05}_{-0.10}) \times 10^{-5}$ has been measured.

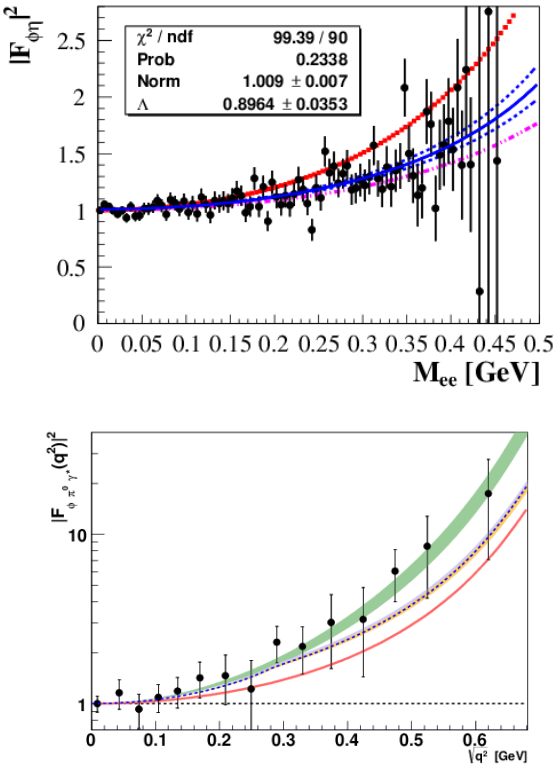

Figure 7. TFF $|F_{\phi P}(q^2)|^2$ as a function of $\sqrt{q^2}$ (invariant mass of e^+e^-) for $\phi \to \eta e^+e^-$ (top) and $\phi \to \pi^0 e^+e^-$ (bottom). Black dots are data. In the top panel the blue curve is the single pole approximation of the TFF with the slope measured on the m_{ee} mass spectrum. Red and purple are different theoretical model: Terschluensen/Leupold [52] and VMD, respectively. In the bottom panel the green band is the Ivashyn model [55], the red curve is the VMD expectation, while the dashed line is the KLOE-2 fit result.

6. η physics

Recently a new result on the $\eta \to \pi^+\pi^-\pi^0$ Dalitz plot density with the highest statistics in the world ($\sim 4.5 \cdot 10^6$ events) [56] has been released. This analysis allows to extract the light quark mass difference and to

perform a test of the charge conjugation violation. The η decay is selected among the $\phi \to \eta\gamma$ radiative decay events having two tracks and two extra gamma's. The density of the Dalitz plot as a function of the kinetic energies of the pions is then fitted with a polynomial:

$$|A(X,Y)|^2 = \mathcal{N}(1 + aY + bY^2 + cX + dX^2 + eXY + fY^3 + gX^2Y + ...) \quad (6)$$

where X and Y are the normalized Dalitz plot variables. The eq. 6 should be symmetric under X parity (charge conjugation) thus resulting in $c = e = 0$, confirmed by data. Fitting the distribution show in fig. 8 KLOE-2 obtained the following results for the non-vanishing coefficients:

$$a = -1.095 \pm 3 \pm 2;\ b = 0.145 \pm 3 \pm 5;\ \mathrm{d} = 0.081 \pm 3^{+5}_{-6};$$

$$\mathrm{f} = 0.141 \pm 7^{+7}_{-8};\ \mathrm{g} = -0.044 \pm 9^{+12}_{-13}$$

The g parameter has been observed different from zero for the first time because of the high statistics collected and high purity of the signal selected.

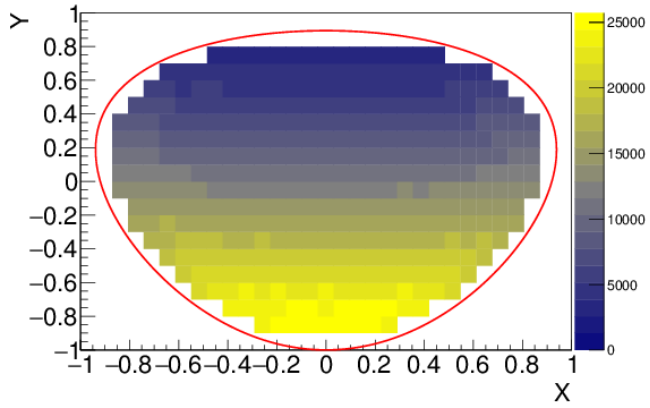

Figure 8. Dalitz density distribution as a function of $X = \sqrt{3}\frac{T_{\pi^+} - T_{\pi^-}}{Q_\eta}$ and $Y = \frac{3T_{\pi^0}}{Q_\eta} - 1$ and $Q_\eta = m_\eta - 2m_{\pi^+} - m_{\pi^0}$.

7. Conclusions

The data delivery progression, shown in fig. 1, demonstrate DAΦNE capabilities to fulfill the KLOE-2 physics run goal within the allocated time. The performance of the collider is constantly monitored in order to guarantee quantity and quality of the data collected.

The KLOE-2 detector is fully functional and all subdetectors are constantly monitored in order to keep the detector fully calibrate and perfectly operational during the whole data taking period.

The KLOE-2 collaboration is still exploiting the old KLOE data-set producing several interesting physics results whit the aim of settle the analysis that could be improved because of the new data taking especially on the $\gamma\gamma$ physics and kaon interferometry.

8. References

[1] G. Amelino-Camelia *et al.*, Eur. Phys. J. C **68** (2010) 619
[2] G. Vignola et al., Frascati Phys. Ser. 4:19-30, 1996.
[3] P. Raimondi et al., arXiV:physics/0702033; C. Milardi et al., Int.J.Mod.Phys.A24:360-368, 2009; M.
[4] C. Milardi et al 2012 JINST 7 T03002.
[5] C. Milardi et al, THPRI002, IPAC14 (2014) .
[6] A. De Santis et al, THPRI015, IPAC14 (2014).
[7] C. Milardi et al, WEOCA03, IPAC14 (2014).
[8] M. Adinolfi *et al.*, [KLOE],NIM A 488 (2002) 51.
[9] M. Adinolfi *et al.*, [KLOE],NIM A 482 (2002) 363.
[10] D. Babusci *et al.*, NIM A **617**, 81 (2010).
[11] F. Archilli, *et al.*, NIM A **617** (2010) 266.
[12] F. Happacher *et al.*, Nucl. Phys. Proc. Suppl. **197**, 215 (
[13] M. Cordelli *et al.*, NIM A **617**, 105 (2010).
[14] A. Balla, *et al.*, NIM A **628** (2011) 194
[15] A. Di Domenico, Frascati Physics Series, Vol. 43 (2007)
[16] A. Einstein, B. Podolsky and N. Rosen, Phys. Rev. **47**, 777 (1935).
[17] V. A. Kostelecky, Phys. Rev. D **64** (2001) 076001
[18] O. W. Greenberg, Phys. Rev. Lett. **89** (2002) 231602.
[19] D. Babusci *et al.* [KLOE-2 Collaboration], Phys. Lett. B **730**, 89 (2014)
[20] A. Di Domenico, JHEP **1510**(2015)139
[21] O. Adriani, et al., Nature 458 (2009) 607.
[22] P. Jean, et al., Astron. Astrophys. 407 (2003) L55.
[23] J. Chang, et al., Nature 456 (2008) 362.
[24] HESS Coll., Phys. Rev. Lett. 101 (2008) 261104.
[25] HESS Coll., Astron. Astrophys. 508 (2009) 561.
[26] A. A. Abdo, et al., Phys. Rev. Lett. 102 (2009) 181101.
[27] R. Bernabei, et al., Int. J. Mod. Phys. D 13 (2004) 2127.
[28] R. Bernabei, et al., Eur. Phys. J. C 56 (2008) 333.
[29] CoGeNT Coll., Phys. Rev. Lett. 106 (2011) 131301.
[30] CoGeNT Coll., Phys. Rev. Lett. 107 (2011) 141301.
[31] AMS Coll., Phys. Rev. Lett. 110 (2013) 141102.
[32] KLOE-2 Coll., Phys. Lett. B 706 (2012) 251255.
[33] KLOE-2 Coll., Phys. Lett. B 720 (2013) 111115.
[34] M. Reece, L. T. Wang, JHEP 07 (2009) 51.
[35] G. C. Feldman, R. D. Cousins, Phys. Rev. D 57 (1998) 3873.
[36] KLOE-2 Coll., Phys. Lett. B 736 (2014) 459464.
[37] L. Barz'e, et al., Eur. Phys. J. C 71 (2011) 1680.
[38] E141 Coll., Phys. Rev. Lett. 59 (1987) 755.
[39] E774 Coll., Phys. Rev. Lett. 67 (1991) 2942.
[40] MAMI/A1 Coll., Phys. Rev. Lett. 106 (2011) 251802.
[41] APEX Coll., Phys. Rev. Lett. 107 (2011) 191804.
[42] WASA Coll., Phys. Lett. B 726 (2013) 187.
[43] HADES Coll., Phys. Lett. B 731 (2014) 265271.
[44] A1 Coll., Phys. Rev. Lett. 112 (2014) 221802.
[45] BaBar Coll., arXiv:1406.2980.
[46] A. R. B. Batell, M. Pospelov, Phys. Rev. D 79 (2009) 115008.
[47] A. Anastasi *et al.*, Phys. Lett. B **750** (2015) 633
[48] A. Anastasi *et al.* [KLOE-2], Phys. Lett. B **757** (2016) 356
[49] A. Anastasi *et al.* [KLOE-2], Phys. Lett. B **747** (2015) 365
[50] F. Jegerlehner, A. Nyffeler, Phys.Rept.477(2009)1
[51] L.G. Landsberg, Phys. Rep.**128**(1985)301.
[52] C. Terschlusen, S. Leupold, Phys. Lett. B**691**(2010)191.
[53] D. Babusci *et al.* [KLOE-2], Phys. Lett. B **742** (2015) 1
[54] A. Anastasi *et al.* [KLOE-2], Phys. Lett. B **757** (2016) 362
[55] S. Ivashyn, Prob. Atomic Sci. Technol. **2012N1**(2012)179.
[56] A. Anastasi *et al.* [KLOE-2 Coll.], JHEP **1605** (2016) 019